A DOUBLE-LAYER CNN FOR IMAGE RESTORATION AND EDGE DETECTION

Simone Naso, Marco Storace, and Mauro Parodi

Department of Biophysical and Electronic Engineering, University of Genoa, Via Opera Pia 11a, I-16145 Genova, ITALY. E-mail: storace@dibe.unige.it

1. Introduction

In this paper, we shall obtain a cellular nonlinear network (CNN) able to implement an approximation of the method proposed by Ambrosio and Tortorelli for image restoration and edge extraction [1]. Ambrosio and Tortorelli, on the basis of the method proposed by Mumford and Shah [2], related the solution of the image-processing problem to the minimization of a proper functional. To solve the image-processing problem means to find two functions (devoted one to image restoration and the other to edge detection) depending on two space variables. As a consequence, the problem can be solved through a two-layer CNN, that allows to find a solution in real time. The CNN will be obtained by applying a Finite Difference Method (FDM) to the variational formulation of the problem, i.e., by properly extending the method defined in References [3,4]. In particular, in [3] the following class $\mathcal{C}$ of functionals F(w(x,y)) has been considered:

$$F(w(x,y)) = \int_\Omega [\Psi(w) + \Phi(\nabla w, H(w))]\,dxdy \qquad (1)$$

where $w(x,y)$: $\Omega \subset \mathbb{R}^2 \to \mathbb{R}$, the term $\Psi(\cdot)$ depends on the function w(x,y) only and the term $\Phi(\cdot)$ depends on the first- and second-order spatial variations of the function w.

The Ambrosio-Tortorelli's method performs image processing by minimizing the following functional:

$$F_\rho(z(x,y),u(x,y)) = \int_\Omega \left[\rho|\nabla u|^2 + \alpha\left(u^2|\nabla z|^2 + \frac{(u-1)^2}{4\alpha\rho}\right) + \beta|z-z_0|^2\right]dxdy \qquad (2)$$

where $\Omega \subset \mathbb{R}^2$ is the image domain, $z(x,y) \in [0,255]$ is the image ($z_0(x,y)$ is the image to be processed), $u(x,y) \in [0,1]$ is a function related to the edges of the image, and α, β, ρ are positive dimensionless parameters. The minimum of this functional (i.e., the functions z(x,y) and u(x,y) that minimize F_ρ) approximates the solution of the Mumford-Shah problem for $\rho \to 0^+$. Taking into account that we are dealing with images, i.e. with functions z(x,y) and u(x,y) that are intrinsically discrete in space, we can (i) dowel the domain Ω into M×N subdomains Ω_{jk} (corresponding to the M×N pixels of the image), (ii) associate the functions z(x,y) and u(x,y) to gray levels z_{jk} and u_{jk}, e.g. through a Finite Difference Method, and (iii) relate them to voltages as follows:

$$v_{zjk} = \eta_z\, z_{jk} \quad , \qquad v_{ujk} = \eta_u\, u_{jk} \qquad (3)$$

where the coefficients η_z and η_u are proper dimensional constants that give the terms v_{zjk} and v_{ujk} in volt.

2. Derivation of the Double-Layer CNN

The functional F_ρ (2) can be easily rewritten as the sum of two terms, one, $F_1(z,u)$, depending on the unknown functions only (local term) and one, $F_2(u,\nabla z,\nabla u)$, depending *also* on their spatial variations (domain term):

$$F_1(z,u) = \int_\Omega \left[\frac{(u-1)^2}{4\rho} + \beta|z-z_0|^2\right]dxdy \qquad (4)$$

$$F_2(u,\nabla z,\nabla u) = \int_\Omega \left[\rho|\nabla u|^2 + \alpha u^2|\nabla z|^2\right]dxdy \qquad (5)$$

Then, the functional F_ρ does not belong to the class (1), but the method proposed in [3] can be easily generalized and applied to it, as we shall see in the following.

After having dowelled the domain Ω into M×N subdomains Ω_{jk}, the *functionals* F_1 and F_2 can be discretized, thus reducing them to *functions* F_{d1} and F_{d2} of 2×M×N variables. The discretization can be obtained, for instance, by resorting to FDM (i.e., by assuming that the unknown functions z(x,y) and u(x,y) hold constant gray-level values z_{jk} and u_{jk} within each subdomain Ω_{jk}). In particular, we shall use a central differences scheme [5], thus obtaining:

$$F_{di}\left(\{z_{jk}\},\{u_{jk}\}\right) = \sum_{j=1}^{M}\sum_{k=1}^{N} F_{ijk}\left(\{z_{jk}\},\{u_{jk}\}\right) \quad i = 1,2 \qquad (6)$$

where

$$F_{1jk} = \frac{\left(u_{jk}-1\right)^2}{4\rho} + \beta\left(z_{jk}-z_{0jk}\right)^2 \qquad (7)$$

and

$$F_{2jk} = \rho\left[\left(\frac{u_{j+1,k}-u_{j-1,k}}{2}\right)^2 + \left(\frac{u_{j,k+1}-u_{j,k-1}}{2}\right)^2\right] + \alpha u_{jk}^2\left[\left(\frac{z_{j+1,k}-z_{j-1,k}}{2}\right)^2 + \left(\frac{z_{j,k+1}-z_{j,k-1}}{2}\right)^2\right] \qquad (8)$$

According to (3), the unknowns z_{jk} and u_{jk} are related to voltages v_{zjk} and v_{ujk}, that can be collected into the column vector $\mathbf{v} = [\mathbf{v_z}^T, \mathbf{v_u}^T]^T$. Then, following the method proposed in [3], the functions F_{d1} and F_{d2} can be related to the (additive) co-content potential functions $\mathcal{G}_1(\mathbf{v})$ and $\mathcal{G}_2(\mathbf{v})$ of two resistive nonlinear networks $\Re_1$ and $\Re_2$, respectively:

$$\begin{aligned}\mathcal{G}_i(\mathrm{v}) &= \eta_F F_{di}\left(\frac{v_z}{\eta_z},\frac{v_u}{\eta_u}\right) = \\ &= \sum_{j=1}^{M}\sum_{k=1}^{N}\eta_F F_{ijk}\left(\frac{v_z}{\eta_z},\frac{v_u}{\eta_u}\right) = \\ &= \sum_{j=1}^{M}\sum_{k=1}^{N}\mathcal{G}_{ijk}(\mathrm{v}) \quad i = 1,2\end{aligned} \tag{9}$$

where the coefficient η_F is a proper dimensional constant that give each term $\mathcal{G}_i$ the physical dimension of a power.

By deriving $\mathcal{G}_{ijk}$ with respect to the components of the vector $\mathbf{v}$, we obtain the equations of a multiterminal resistor $\Re_{ijk}$. By properly connecting the M×N elements $\Re_{ijk}$ (i = 1,2), one obtains the nonlinear resistive network $\Re_i$. The structure of the resistive interconnections between the two layers ("z" and "u") of the resulting CNN is shown in figure 1.

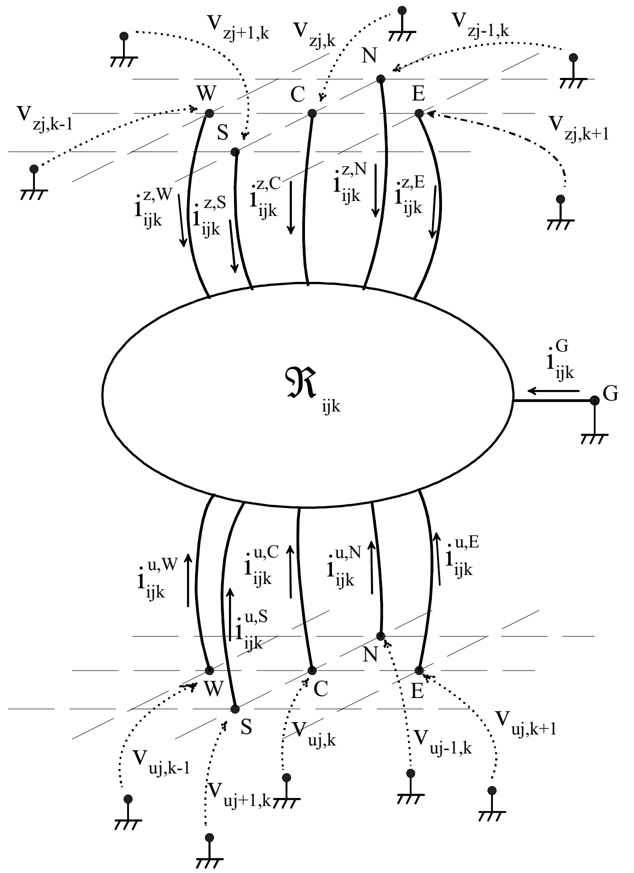

Figure 1. Detail of the interconnections between the two layers of the CNN through the multiterminal resistors $\Re_{1jk}$ and $\Re_{2jk}$.

A further insight to the structure of $\Re_{1jk}$ and $\Re_{2jk}$ is now needed. The constitutive equations of $\Re_{1jk}$ follow directly from $\mathcal{G}_{1jk}$:

$$\begin{cases} i_{1jk}^{z,C} = \dfrac{\eta_F}{\eta_z^2}2\beta\left(v_{zj,k} - v_{0j,k}\right) \\ i_{1jk}^{u,C} = \dfrac{\eta_F}{\eta_u^2}\dfrac{1}{2\rho}\left(v_{uj,k} - 1\right) \\ i_{1jk}^{G} = -\left(i_{1jk}^{z,C} + i_{1jk}^{u,C}\right) \end{cases} \tag{10}$$

A possible circuit interpretation of $\Re_{1jk}$ is proposed in figure 2. As $\mathcal{G}_{1jk}$ depends on v_{zjk} and v_{ujk} only, $\Re_{1jk}$ has three terminals.

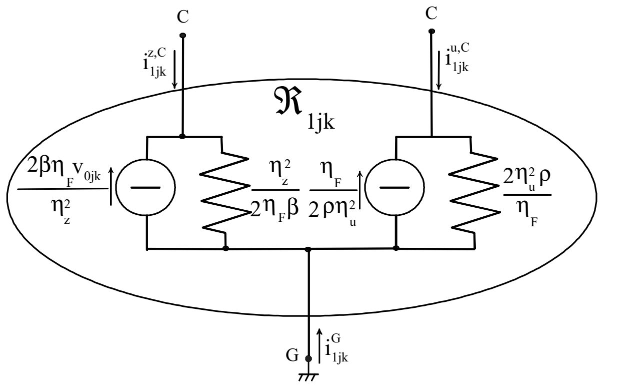

Figure 2. Possible circuit interpretation of the multiterminal resistor $\Re_{1jk}$.

In a completely analogous way, we can derive the constitutive equations of $\Re_{2jk}$. Such equations can be divided up into three subsets, two of which correspond to the multiterminal resistors $\Re_{2jk}^{(I)}$ (eqs. (11)) and $\Re_{2jk}^{(II)}$ (eqs. (12)) shown in figure 3:

$$\begin{cases} i_{2jk}^{z,E} = \dfrac{\eta_F}{\eta_u^2\eta_z^2}\dfrac{\alpha}{2}\left(v_{zj,k+1} - v_{zj,k-1}\right)v_{uj,k}^2 \\ i_{2jk}^{z,W} = -\dfrac{\eta_F}{\eta_u^2\eta_z^2}\dfrac{\alpha}{2}\left(v_{zj,k+1} - v_{zj,k-1}\right)v_{uj,k}^2 \\ i_{2jk}^{u,C(I)} = 2\dfrac{\eta_F}{\eta_u^2\eta_z^2}\alpha v_{uj,k}\left(\dfrac{v_{zj,k+1} - v_{zj,k-1}}{2}\right)^2 \\ i_{2jk}^{G(I)} = -\left(i_{2jk}^{z,E} + i_{2jk}^{z,W} + i_{2jk}^{u,C(I)}\right) \end{cases} \tag{11}$$

$$\begin{cases} i_{2jk}^{z,S} = \dfrac{\eta_F}{\eta_u^2\eta_z^2}\dfrac{\alpha}{2}\left(v_{zj+1,k} - v_{zj-1,k}\right)v_{uj,k}^2 \\ i_{2jk}^{z,N} = -\dfrac{\eta_F}{\eta_u^2\eta_z^2}\dfrac{\alpha}{2}\left(v_{zj+1,k} - v_{zj-1,k}\right)v_{uj,k}^2 \\ i_{2jk}^{u,C(II)} = 2\dfrac{\eta_F}{\eta_u^2\eta_z^2}\alpha v_{uj,k}\left(\dfrac{v_{zj+1,k} - v_{zj-1,k}}{2}\right)^2 \\ i_{2jk}^{G(II)} = -\left(i_{2jk}^{z,S} + i_{2jk}^{z,N} + i_{2jk}^{u,C(II)}\right) \end{cases} \tag{12}$$

The third set of equations follows directly from the quadratic dependence of $\mathcal{G}_{2jk}$ on the pertinent voltage differences (see equations 8 and 9) and corresponds to two linear resistors (see figure 3). The nonlinear resistive network $\Re_2$ is obtained by properly connecting the M×N elements $\Re_{2jk}$.

A stationary point for $\mathcal{G}(\mathbf{v}) = \mathcal{G}_1(\mathbf{v}) + \mathcal{G}_2(\mathbf{v})$ (i.e., a point where $\nabla_{\mathbf{v}}\mathcal{G} = \mathbf{0}$) corresponds to an approximate solution of the original problem. We point out that, even if the original problem is stationary (i.e., its solution does not depend on time), its approximate solution by circuits is regarded as an equilibrium state of the dynamic process related to the system of nonlinear ordinary differential equations $\nabla_{\mathbf{v}}\mathcal{G} = -CI_{2\times M\times N}d\mathbf{v}/dt$ (2×M×N is the size of the identity matrix $I_{2\times M\times N}$). In other words, we make the voltages v_{zjk} and v_{ujk} state variables, by properly connecting 2×M×N linear capacitors C to the networks $\Re_1$ and $\Re_2$, respectively.

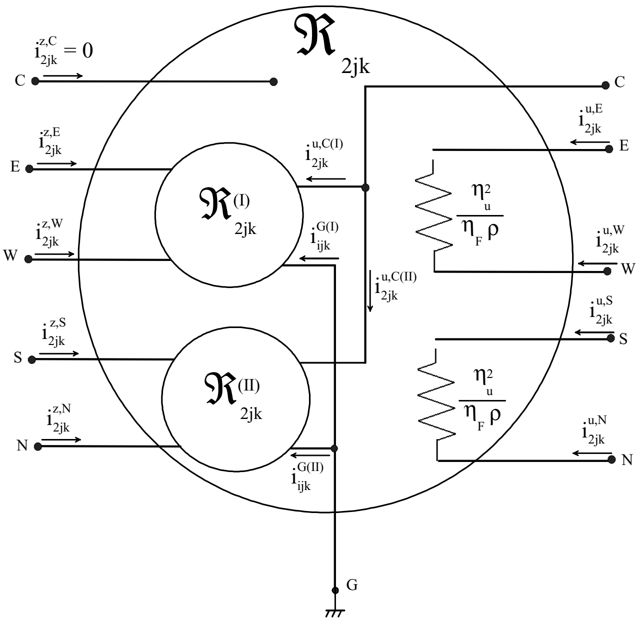

Figure 3. Possible circuit interpretation of the multiterminal resistor $\Re_{2jk}$.

At this point of the synthesis procedure, then, we have two sets of nonlinear equations $dv_{zjk}/dt = f_{zjk}$ and $dv_{ujk}/dt = f_{ujk}$. The nonlinear function f_{zjk} (f_{ujk}) is uniquely defined for any j,k and, generally speaking, contains an addend depending on the state variable v_{zjk} (v_{ujk}) and an addend depending on the state variables v_{zpq} and v_{upq} of the neighborhood set of the jk-th cell; the number of elements of the neighborhood set is a consequence of the adopted discretization scheme (in our case, for the central differences discretization scheme, the neighborhood set contains four elements). These two sets of equations define a double-layer CNN. Each equation can be interpreted as KCL equation involving the jk-th capacitor of a layer and the multi-terminal resistors connected to it (see figure 4 for a detail).

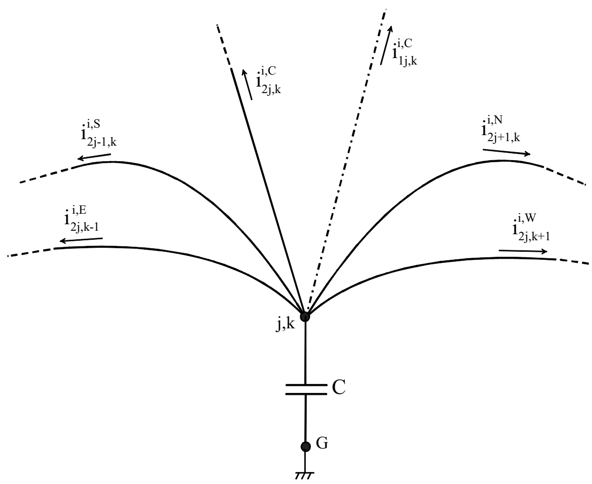

Figure 4. Detail of the jk-th node of one layer of the CNN (i = z,u).

Then, the resulting CNN follows rather directly from the co-content additivity property and from the interpretation of the nonlinear ordinary differential equations in terms of Kirchhoff's equations [4].

A non trivial aspect which is not addressed in this paper concerns the synthesis of the nonlinear multiterminal resistors $\Re_{2jk}^{(I)}$ and $\Re_{2jk}^{(II)}$. A synthesis procedure based on the piecewise-linear approach developed by Julián *et al.* in the last few years [6] has been defined in [7-9].

3. Simulation Results

In this section we shall present some numerical results, obtained by simulating the CNN derived in the previous section. The CNN parameters were fixed to the following values: $\alpha = 15\cdot10^{-3}$, $\beta = 6\cdot10^{-3}$, $\rho = 10^{-2}$ (this choice of the Ambrosio-Tortorelli's model parameters guarantees a good image processing), $\eta_F = 13\cdot10^{-6}$W, $\eta_z = 1/255$V, $\eta_u = 1$V, and C = 10nF.

Figures 1(a,b) show the original image (512×512 pixels) and its noisy version (corrupted with null-mean Gaussian noise, with variance $\sigma = 15$, signal-to-noise ratio = 17.3dB), respectively. The CNN simulation results are reported in figures 1(c,d). In particular, figure 1c shows the restored image (signal-to-noise ratio = 21.3dB), corresponding to u(x,y), i.e., to the voltages v_{ujk} on the capacitors of the layer "u" of the CNN after about 60μs. Figure 1d shows the detected edges, corresponding to z(x,y), i.e., to the voltages v_{zjk} on the capacitors of the layer "z" of the CNN.

Acknowledgments

This work was supported by the MIUR, within the framework of the national research project no. 2001095333_005 "Cellular circuits and algorithms for parallel processing of images," and by the University of Genoa.

(a)

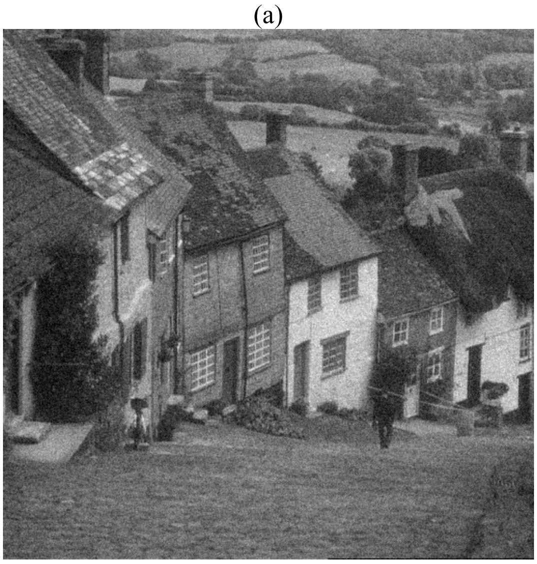

(b)

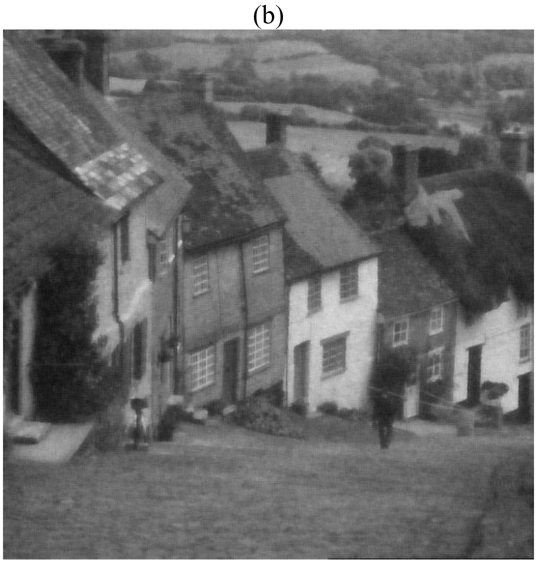

(c)

(d)

Figure 5. (a) Noiseless image and (b) image to be processed (corrupted with null-mean Gaussian noise, with variance σ = 15). CNN simulation results: (c) restored image and (d) detected edges.

References

[1] Ambrosio L., Tortorelli V.M. On the approximation of free discontinuity problems. *Bollettino U.M.I.* 1992; **6-B**: 105-123.

[2] Mumford D., Shah J. Optimal approximations by piecewise smooth functions and associated variational problems. *Comm. Pure Appl. Math. 1989*; **17**: 577-685.

[3] Storace M., Bizzarri F., Parodi M. Cellular non-linear networks for minimization of functionals. Part 1: Theoretical aspects. *International Journal of Circuit Theory and Applications* 2001; **29** (2):151-167.

[4] Bizzarri F., Storace M., Parodi M. Cellular non-linear networks for minimization of functionals. Part 2: Examples. *International Journal of Circuit Theory and Applications* 2001; **29** (2): 169-184.

[5] Abramovitz M., Stegun I.A. *Handbook of Mathematical Functions with Formulas, Graphs, and Mathematical Tables*, Wiley, New York, 1972.

[6] Julián P., Desages A., D'Amico B. Orthonormal high level canonical PWL functions with applications to model reduction. *IEEE Transactions on Circuits and Systems – I* 2000; **47**: 702-712.

[7] Storace M., Julián P., Parodi M. Synthesis of nonlinear multiport resistors: a PWL approach. *IEEE Transactions on Circuits and Systems – I* 2002; **49**: in press.

[8] Storace M., Repetto L., Parodi M. A method for the approximate synthesis of cellular nonlinear networks - Part 1: Circuit definition. *International Journal of Circuit Theory and Applications*: in press.

[9] Repetto L., Storace M., Parodi M. A method for the approximate synthesis of cellular nonlinear networks - Part 2: Circuit reduction. *International Journal of Circuit Theory and Applications*: in press.